Unusual Spectrally Reproducible and High Q-Factor Random Lasing in Polycrystalline Tin Perovskite Films

Vladimir S. Chirvony,* Isaac Suárez, Jesus Sanchez-Diaz, Rafael S. Sánchez, Jesús Rodríguez-Romero, Iván Mora-Seró,* and Juan P. Martínez-Pastor*

An unusual spectrally reproducible near-IR random lasing (RL) with no fluctuation of lasing peak wavelength is disclosed in polycrystalline films of formamidinium tin triiodide perovskite, which have been chemically stabilized against Sn^{2+} to Sn^{4+} oxidation. Remarkably, a quality Q-factor as high as $\approx 10^4$ with an amplified spontaneous emission (ASE) threshold as low as $2~\mu J~cm^{-2}$ (both at 20 K) are achieved. The observed spectral reproducibility is unprecedented for semiconductor thin film RL systems and cannot be explained by the strong spatial localization of lasing modes. Instead, it is suggested that the spectral stability is a result of such an unique property of Sn-based perovskites as a large inhomogeneous broadening of the emitting centers, which is a consequence of an intrinsic structural inhomogeneity of the material. Due to this, lasing can occur simultaneously in modes that are spatially strongly overlapped, as long as the spectral separation between the modes is larger than the homogeneous linewidth of the emitting centers. The discovered mechanism of RL spectral stability in semiconductor materials, possessing inhomogeneous broadening, opens up prospects for their practical use as cheap sources of narrow laser lines.

V. S. Chirvony, J. P. Martínez-Pastor
UMDO
Instituto de Ciencia de los Materiales
Universidad de Valencia
Valencia 46980, Spain
E-mail: vladimir.chyrvony@uv.es; juan.mtnez.pastor@uv.es
I. Suárez
Escuela Técnica Superior de Ingeniería
Universidad de Valencia
Valencia 46100, Spain
J. Sanchez-Diaz, R. S. Sánchez, I. Mora-Seró
Institute of Advanced Materials (INAM)
Universitat Jaume I
Castelló de la Plana, Castelló 12006, Spain
E-mail: sero@uji.es
J. Rodríguez-Romero
Facultad de Química
Universidad Nacional Autónoma de México
Coyoacán, Ciudad de México 04510, Mexico

1. Introduction

A random laser is a special type of laser where the optical feedback is provided by multiple scattering inside a medium providing an optical gain. It is important to emphasize that the random lasing (RL) phenomenon comprises two distinctively different subfields, which are often named as "incoherent feedback" and "resonant feedback" RL.[1–4] In the case of incoherent feedback, multiple scattering prevents light from leaving the optically pumped region (usually of linear size of tens to hundreds μm), and it turns out that such a disorder-induced feedback is sufficient for a dramatic narrowing (down to a few nm) of the emission spectrum, above a certain excitation fluence threshold.[3] Suspensions of colloidal particles in organic dye solutions, powder grains of laser crystal materials and π-conjugated polymer films were mainly used to produce incoherent feedback RL.[2,3] On the contrary, a quite different scenario is found in the case of the resonant feedback RL, which consists in a disorder-induced localization of the photonic modes in a small space, with size comparable to the wavelength of the optical mode.[4] As a result of the light interference in the presence of strong scattering and gain, a number of very sharp laser-like lines, with a full width at half maximum (FWHM) of the order of ≈ 0.1–0.2 nm, emerge in the emission spectrum. Such resonant type of RL was observed for the first time in 1998 for systems where the gain and multiple scattering were provided by the same material (ZnO and GaN polycrystalline semiconductor films and powders).[5,6] For sake of clarity from now on, a more widespread nomenclature will be employed, in which incoherent and resonant feedback RL will be referred as amplified spontaneous emission (ASE) and RL, respectively. In most of the cases, RL is keep just a curiosity due to the impossibility of being technologically exploited mainly owing to the spectral fluctuation of the laser peaks.

In this context, lead halide perovskites (Pb-HPs) are excellent materials for lasing because they are direct gap semiconductors[7,8] with very sharp optical absorption edge, whose absorption coefficient exceeds $10^4~cm^{-1}$ just above the band edge.[9] Since the first discovery of ASE[10] and RL[11] in Pb-HP films in 2014, dozens of works that report these phenomena have been published.[12,13] It should be noted, however, that the

**ADVANCED
SCIENCE NEWS**

www.advancedsciencenews.com

**ADVANCED
MATERIALS**

www.advmat.de

vast majority of these works report on the RL observation only when external strongly scattering elements are introduced in Pb-HP films, and only in a few of them, the faces of the crystal grains that constitute the spin-coated polycrystalline thin films, were responsible for the RL.[14–18] Hence, the need of external scattering elements to induce the RL effect can apparently be interpreted as a result of insufficiently efficient scattering in pristine polycrystalline Pb-HP films.

Apart from lasing characteristics and quality issues, the presence of the hazardous Pb of Pb-HP derivatives makes their exploitation in an industrial scale unpromising. Therefore, an important current task is the development of laser media based on Pb-free halide perovskites, which are safer compounds compatible with relatively simple and straightforward fabrication methods and with similar emission efficiencies as their lead-containing counterparts. Among them, tin-based halide perovskites (Sn-HPs) are, probably, the most promising candidates to substitute Pb-HPs due to their interesting semiconductor attributes and the recent progress achieved in the development of highly-efficient optoelectronic devices.[19,20] Despite this, optical studies on Sn-HPs are indeed scarce because of the lower reported stability in comparison with Pb-HPs, mostly due to the detrimental Sn^{2+} to Sn^{4+} oxidation that spoils the material's properties. To the best of our knowledge, Sn-HPs lasing has been observed only in two precedents,[21,22] but only in one of them the RL regime was achieved for a pristine polycrystalline film without the insertion of any external scattering elements,[22] albeit with a very high lasing threshold of 18 mJ cm^{-2} and spectrally non-reproducible lasing modes.

Recently, we have achieved a dramatic increase in the stability and overall performance of Sn-HPs through the introduction of an anti-oxidant agent (NaBH$_4$) and a passivating additive, dipropylammonium iodide (DipI), applied in Sn-HPs solar cells.[23] In our recently published work[24] and in the present manuscript, we take advantage of this outstanding chemical engineering approach to carry out an extensive exploration of ASE and RL effects in polycrystalline formamidinium tin triiodide perovskite (FASnI$_3$) thin films without addition of any external scattering elements. Indeed, using such a chemically stabilized material, we achieved very low ASE thresholds of 100 nJ cm^{-2} and 1 μJ cm^{-2} for polycrystalline FASnI$_3$ films in waveguides based on both, rigid (Si/SiO$_2$) and flexible (polyethylene terephthalate) substrates, respectively.[24] Remarkably, here we unprecedentedly identified that polycrystalline FASnI$_3$ is an excellent material for RL, which combines an extremely high optical gain together with a strong scattering efficiency. The films characterized in backscattering geometry yielded an ASE threshold as low as 2 μJ cm^{-2} at 20 K together with the appearance of very narrow lines, which are characteristic of the RL. The FWHM of the RL lines are in the order of $\Delta\lambda \approx 0.1$ nm at emission wavelength $\lambda \approx 900$ nm, which results in a quality factor Q ($\omega_r/\Delta\omega = \lambda_r/\Delta\lambda$, where ω_r stands for the spectral position of the resonance) as high as 10^4. Nevertheless, the most unexpected and at the same time outstanding property of pristine polycrystalline FASnI$_3$ films was the extremely high spectral stability of the generated RL modes, in contrast to chaotic changes of the modes spectral positions in the case of thin film semiconductors in general and in similar Pb-HP films in particular. Based on statistical analysis of the RL mode spacing distribution, we conclude that the lasing modes are in the *spectral repulsion regime* that arises from the very strong inhomogeneous broadening of the emitting centres, which is a characteristic of FASnI$_3$ films. The discovered effect of self-stabilization of RL lines in Sn-HP films opens up prospects for their practical use as cheap sources of narrow laser lines.

2. Results

The FASnI$_3$ films used in the present work are grown by using a precursor solution of SnI$_2$, FAI, SnF$_2$, DipI, and NaBH$_4$ in a DMSO:DMF solvent mixture, see details in Supporting Information. After the film deposition, typically 200 nm thick, onto the glass substrate, a 3-days light-soaking treatment, using white LED lamp, was applied inside a N$_2$ filled glovebox, as such light soaking has proven beneficial in photo-reducing Sn^{2+} to Sn^{4+}, increasing the film photovoltaic performance.[23] The SEM image of the film, see **Figure 1**a, reveals a dense package of grains, whose size distribution can be well fitted by a Gaussian contour with a maximum at ≈800 nm, see Figure 1b.

Typical room temperature absorption as well as room and low temperature photoluminescence (PL) spectra of these optimized FASnI$_3$ thin films deposited on glass are shown in Figure 1c. As it turned out, spectral positions of the PL spectra may vary somewhat, depending on the location of excitation on the sample, especially at low temperature. For the same sample, PL maximum can lie in the range of 875–895 nm at room temperature and 925–965 nm at 20 K, while the FWHM is typically ≈110 meV at room temperature and can be 50–100 meV at 20 K, see Figure S1a (Supporting Information) for details. The reasons for such inhomogeneity of FASnI$_3$ films, as well as very large FWHM values at low temperatures, will be discussed below.

PL lifetime ($\tau \approx 1.40$ ns) remains practically unchanged with temperature, see Figure 1d and Figure S1 (Supporting Information). Despite this lifetime may not seem significantly high, it is worth highlighting that it represents an increase of near 200% as compared to the pristine FASnI$_3$, i.e., without DipI and NaBH$_4$ additives, nor light-soaking treatment.[23] Some general information about the photophysics of Sn-based iodide perovskites explaining short PL lifetimes is given in Note S1b (Supporting Information).

To study ASE and RL effects, FASnI$_3$ films were excited by 1-ns laser pulses at 532 or 355 nm and PL signal was detected in backscattering geometry to investigate lasing properties. Two different excitation spot sizes were used, a "large" elliptic spot (420 × 100 μm in size) and a "small" circular spot (100 μm in diameter), see Scheme S1 and Note S1 in Supporting Information for more details. **Figure 2**a shows PL spectra of a FASnI$_3$ thin film on glass measured at 20 K with excitation by 1-ns pulses at 355 nm at different excitation fluencies in a large-spot excitation regime. Figure 2a reveals that a rather broad, 30–40 nm FWHM, spontaneous PL band is observed at the lower excitation fluencies; however, upon reaching a fluence of ≈2 μJ cm^{-2}, the PL spectrum narrows down to ≈5 nm FWHM. Such a narrow band is identified as ASE, which experiences a superlinear growth of intensity with the excitation fluence, see Figure 2b. Moreover, for the highest excitation energy values
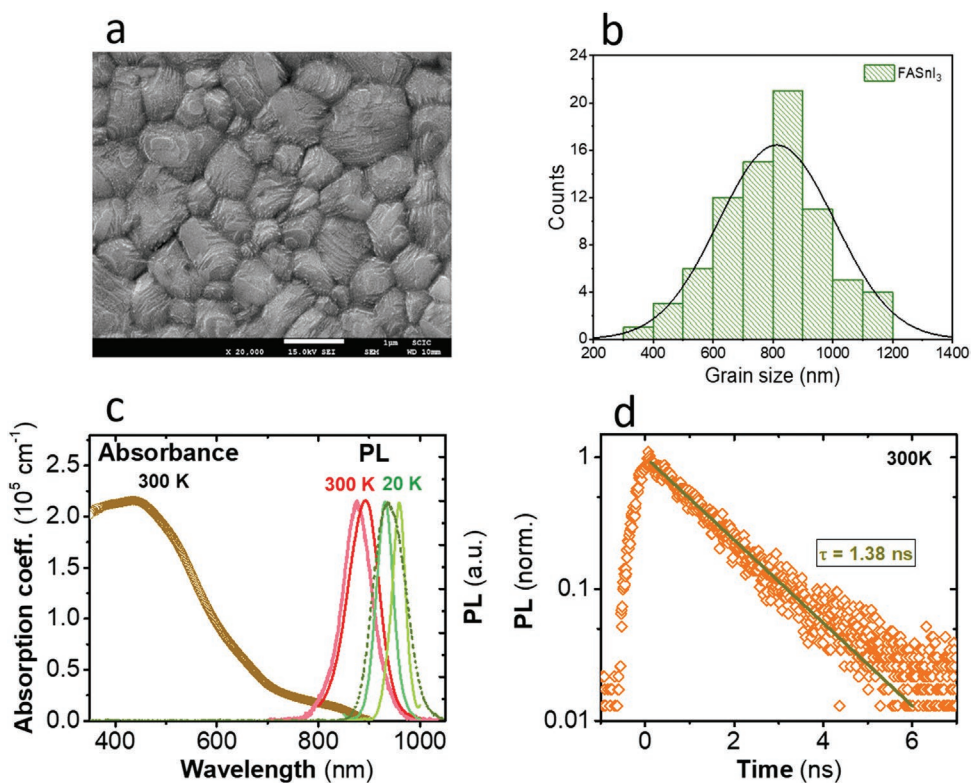
Figure 1. Morphological and optical characteristics of FASnI$_3$ film on glass, thickness ≈200 nm: a) SEM image; b) grain size distribution, scale bar is 1 µm; c) typical room temperature absorption as well as room (red lines) and low temperature (green lines) PL spectra, PL maxima positions and FWHM of which are depending on the excitation spot location on a sample; d) PL decay kinetics.

(>10 µJ cm^{-2}) the ASE band is evidently modulated by narrow peaks that could be attributed to RL modes, see below. The log–log curve of the PL band intensity as a function of the excitation fluence, see Figure 2b, shows the three-stage (S-shaped) behavior that is a typical characteristic of lasing. Each stage can be fitted by power low function $I_{PL} = (I_{exc})^k$, where I_{PL} is the emitted light intensity and I_{exc}, is the excitation fluence. The first stage with the k-slope close to unity indicates the characteristic behavior of the spontaneous emission. Then, at excitation fluencies comprised within 2 and 10 µJ cm^{-2}, the dependence is

characterized by $k > 2$ that is a sign of the stimulated emission, ASE regime. Finally, in the 10–50 µJ cm^{-2} excitation diapason, k again becomes close to 1, which is a signature of the lasing regime.[25] The same value of the ASE threshold at 20 K, $\Phi_{thr} \approx 2$ µJ cm^{-2}, was found for excitation under 1-ns pulses at 532 nm, see Figure S2 (Supporting Information). It is interesting to note that FASnI$_3$ films, which were fabricated with additives in the same conditions, but without post-synthetic light-soaking procedure, exhibited a higher ASE threshold of about 4–5 µJ cm^{-2}, see Figure S3 (Supporting Information).
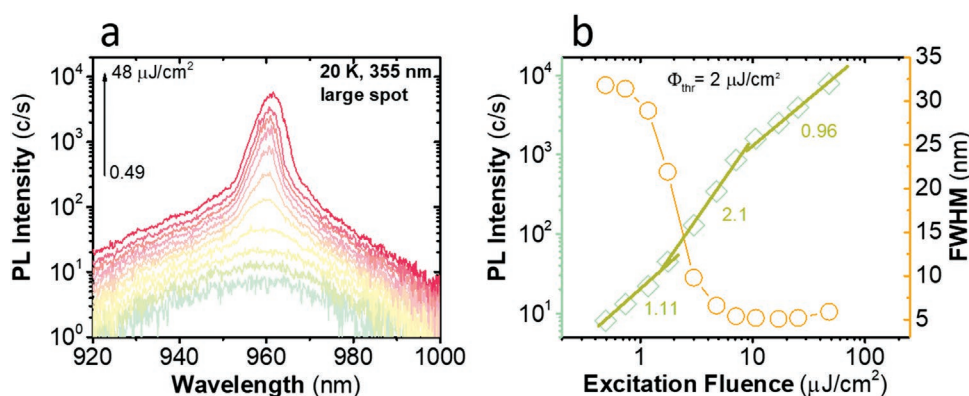
Figure 2. a) PL spectra of FASnI$_3$ thin film on glass measured at 20 K at different excitation fluences at 355 nm; b) log–log presentation of PL intensity (rhombuses) and FWHM (circles) dependencies on the excitation fluence, from which ASE threshold $\Phi_{thr} = 2$ µJ cm^{-2} is determined.
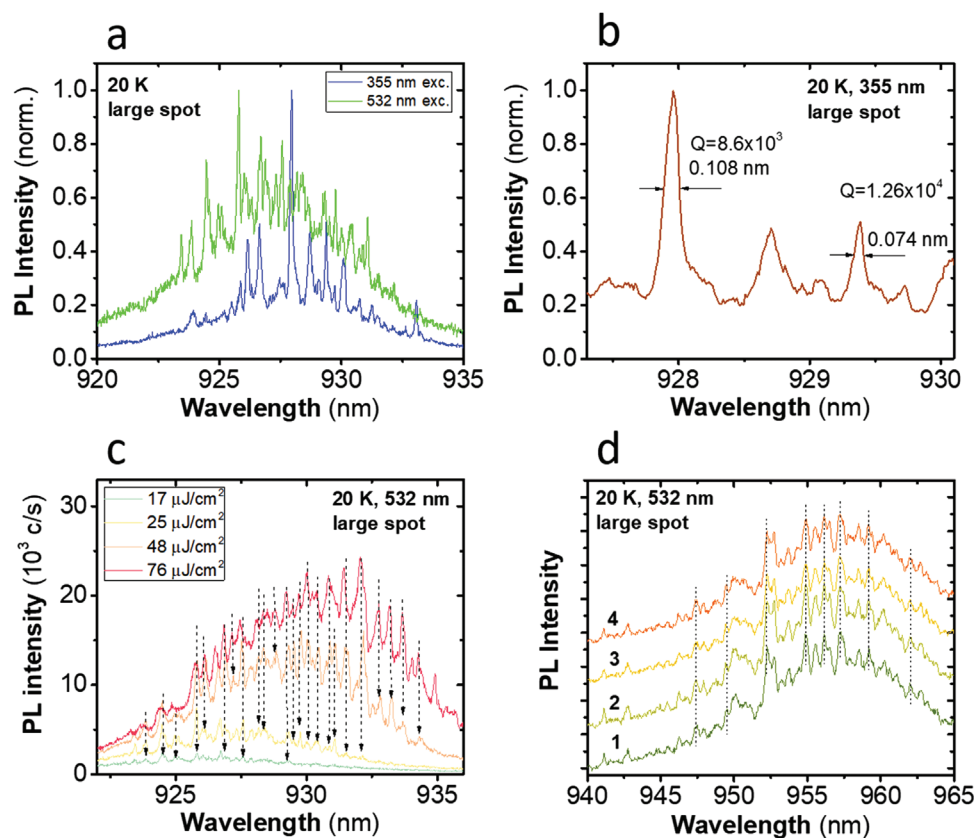
Figure 3. Typical ASE/RL spectra of FASnI$_3$ films on glass measured at 20 K: a) comparison of spectra measured after 355 nm and 532 nm excitation; b) zoomed spectrum from (a) measured after 355 nm excitation; c) spectra measured with increasing excitation fluence at 532 nm; d) ASE/RL spectra 1 – 4 measured with a one-minute interval after each other with a constant excitation fluence. Vertical dashed lines are eye guides to demonstrate that there is no shift among the RL peaks.

This evidences that the radiative recombination of the exciton is remarkably enhanced upon the light soaking, that photoreduces part of Sn^{4+} into Sn^{2+}, in agreement with our previous work.[23] Finally, the ASE threshold found at room temperature was 35–40 μJ cm^{-2}, around one order of magnitude higher than that at 20 K, see Figure S4 (Supporting Information).

A closer examination of the light emission spectra presented in Figures 2, complemented further examples in Figures S2–S4 (Supporting Information) show that, at excitation fluences slightly exceeding the ASE threshold, very narrow lines (spikes) emerge on top of the ASE contour. The corresponding PL spectra, which were obtained with excitation wavelengths of 355 and 532 nm, and approximately equal excitation fluence of ≈25 μJ cm^{-2}, are identified as a result of random lasing,[4,26] see **Figure 3a**. The spectra are characterized by narrow RL lines rising above the ASE (Lorentzian) contours. Interestingly, the relative intensity of narrow RL lines respect to ASE contour in spectra measured at 355 nm excitation, is systematically higher as compared to those obtained upon 532 nm excitation. We believe that this effect is caused by: i) the lower refractive index of the material at 355 nm that decreases the part of the excitation light reflected by the surface, thus increasing the transmitted part of the incident light,[27] and ii) the higher absorption coefficient of the FASnI$_3$ at 355 nm versus 532 nm; both factors contribute to the growth of gain for the shorter excitation wavelength.[27]

Our evaluation of the lasing quality factor Q of our RL lines at 20 K is shown in Figure 3b. The lowest FWHM value of RL lines excited by 355 nm pulses is ≈0.1 nm, that corresponds to a quality factor Q as high as ≈10^4 at ≈900 nm. Remarkably, the lowest FWHM values obtained for our RL lines at room temperature were of ≈0.2–0.4 nm that correspond to a Q ≈2–4 × 10^3 (not shown). Note that even though these values, which are obtained for the random lasing system without any preset resonator, are lower than those obtained for resonators supporting whispering gallery modes, where Q factor is usually 10^4–10^5,[30,31] their magnitude is very high and generally comparable to those measured for conventional cavities such as Fabry–Perot resonators, where Q factor is usually 10^3–10^4.[28,29] It is worth highlighting that the above ASE and RL parameters obtained for FASnI$_3$ are superior to those known for all previously studied pristine Pb-based films,[14,16,18,32] for which ASE threshold values range from ≈10 μJ cm^{-2} [16] to ≈50 mJ cm^{-2} [18] and Q-factor values from < 10^3 to 7 × 10^3.[18]

Another interesting effect that we observed under the large spot excitation conditions, is the shift of the ASE contour toward the longer-wavelength region with increasing excitation fluence, see Figure 3c. We suggest that this effect is a consequence of the fact that the excitation energy increase is accompanied by an increase of the effective excitation spot size at a fixed excitation intensity level, see Figure S5 (Supporting Information).

**ADVANCED
SCIENCE NEWS**

www.advancedsciencenews.com

**ADVANCED
MATERIALS**

www.advmat.de

As a result, at higher excitation fluences the ASE radiation travels along a longer path, which in turn causes stronger re-absorption and re-emission of the emitted light, and therefore a bathochromic shift of the ASE contour is induced.[33] Nevertheless, despite this ASE contour red shift, the spectral position of practically all the RL lines remains unchanged with the excitation fluence, see Figure 3c. The position of the RL lines also does not change in time with a constant excitation fluence, see Figure 3d. Like in the low temperature case, the room temperature RL spectra also demonstrate spectral reproducibility at constant excitation fluence as well as when the fluence experiences 3–5 fold changes, see Figure S5b (Supporting Information).

Note also that some photodegradation of FASnI$_3$ films was detected upon excitation with 355 nm light pulses, which manifested itself by a permanent blue shift of the RL spectrum as a whole with the shift rate of ≈0.1 nm per minute at excitation fluences of tens µJ cm^{-2}. We attribute this shift to the photodegradation of the material and a change (decrease) in its refractive index. In case of excitation by 532 nm pulses, the rate of the short-wavelength shift decreases by ≈10 times at similar fluences, which makes it possible to neglect it during operation for tens of minutes to an hour.

It is known that size and even shape of the excitation spot can greatly influence a RL spectrum.[1] We assumed that the elliptical shape of the large excitation spot with the larger axis as long as 420 µm can be responsible for the dominance of ASE component in the observed spectra and relatively low contribution of RL narrow lines. This suggestion is based on the simple idea that the formation of ASE spectra requires a sufficiently large size of an excited region to generate ASE. It is well-known that the intensity of light, I, in a medium with optical gain, g, grows exponentially with the path length, z, i.e., $I \propto e^{g \cdot z}$, hence the amplified signal becomes smaller for short paths. To check this hypothesis, we switched to a smaller circular spot, 100 µm in diameter, for the excitation of FASnI$_3$ samples, and a clear drastic variation of the PL spectra structure was observed compared to that obtained for the larger spot, see **Figure 4**. First, with an increase of the excitation fluence narrow RL lines appear directly on top of the broad spontaneous luminescence contour with a strongly reduced intensity of the ASE contour. Spectral positions of the narrow RL lines do not change even when the pump fluence varies by an order of magnitude, see Figure 4a. The spectra shown in Figure 4a are presented in Figure 4d in the normalized form. As one can see, at the lowest excitation intensities about a dozen of narrow RL lines emerge in the center of the spontaneous emission contour. With an increase of the excitation energy, additional lines appear at the edges of the spectrum, so that at the maximum pump energies used, the number of lines increases to ≈30. It is well seen in Figure 4d that the spectral positions of the lines and their profiles do not change with excitation fluence, as it was also observed in Figure 3c. Specific experiments were also carried out to determine the stability of the RL spectra at constant pumping, which confirmed the invariance of the spectral position of the laser modes with time, during at least one hour of measurements, only some changes in the relative intensities of different modes were observed, see Figure 4b.

Therefore, a comparison of the PL spectra obtained with a large and small excitation spot suggests that the broad ASE band and the spectrum consisting of narrow RL lines are formed in parallel and independently of each other due to two different mechanisms. For the formation of ASE, a sufficient size of the exciting spot is required: we observe that for 100 µm excitation spot ASE intensity is very low as compared to the intensity of RL lines, but for 400 µm spot ASE is of high intensity and even prevails. In both cases the spectrally narrow RL modes continue to be efficiently generated and, noticeably in this work, remain spectrally reproducible.

Due to the high Q values of the observed RL lines and their extremely high spectral stability, we were able to investigate optical parameters of the system at the level of individual RL lines. Figure 4c displays the dependence of the intensity of several individual lines with the excitation fluence. The corresponding spectra are shown in Figure S6 (Supporting Information), where the analyzed lines are marked with asterisks. As in case of ASE contours excited with a large excitation spot, see Figure 2b, S-like dependences are observed for all three selected RL lines with similar thresholds of ≈100 µJ cm^{-2}, see Figure 4c. The data presented in Figure 4c shed light on gain dynamics and the interaction between lasing and optical pumping in our RL system by evaluation of the so called β factor. By definition, β is the fraction of spontaneous radiation that does contribute to a given lasing mode.[34] The fitting with standard laser rate equations, solid line in Figure 4c,[35] revealed that this factor lays in the interval $\beta = 0.01–0.05$. This remarkable low value of β is due to the fact that the emitted light is distributed along the different modes that compose the spectra.

To emphasize the unique properties of RL spectra of polycrystalline FASnI$_3$ films, we investigated ASE and RL generated in polycrystalline films of widely studied Pb-HPs, CH$_3$NH$_3$PbI$_3$ (MAPbI$_3$), in order to compare the behavior of the two materials under identical excitation conditions. Figure S7 (Supporting Information) shows a SEM image and grain size distribution of a typical MAPbI$_3$ film. Figure S8 (Supporting Information) demonstrates RL spectra of MAPbI$_3$ films detected at 20 K with a large spot excitation. Unlike FASnI$_3$, for MAPbI$_3$ films RL lines are practically not observed under 532 nm excitation and are of very low relative intensity under 355 nm excitation. In addition, the spectral positions of the RL lines of MAPbI$_3$ films do not demonstrate stability, changing with time, see Figure S8b (Supporting Information). The quality of RL in MAPbI$_3$ films does not improve after switching to small spot excitations: only ASE contour is observed with an increase in the excitation fluence in MAPbI$_3$ films, for both large and small excitation spots, see Figure S9 (Supporting Information), whereas in FASnI$_3$ films RL lines are clearly visible for a large excitation spot and completely dominate for a small one. Generally, a similar trend of full absence of RL lines in MAPbI$_3$ films for both excitation spot sizes is observed at room temperature in contrast with the clear observation for FASnI$_3$, see Figure S10 (Supporting Information).

We also performed a statistical analysis of mode spacing in RL spectra of FASnI$_3$ measured at low and high temperatures, 20 and 300 K respectively, with use of a large and small excitation spots, Figure 5 a–d. A very important observation is that the average mode spacing does not vary among FASnI$_3$

ADVANCED
SCIENCE NEWS

www.advancedsciencenews.com

ADVANCED
MATERIALS

www.advmat.de
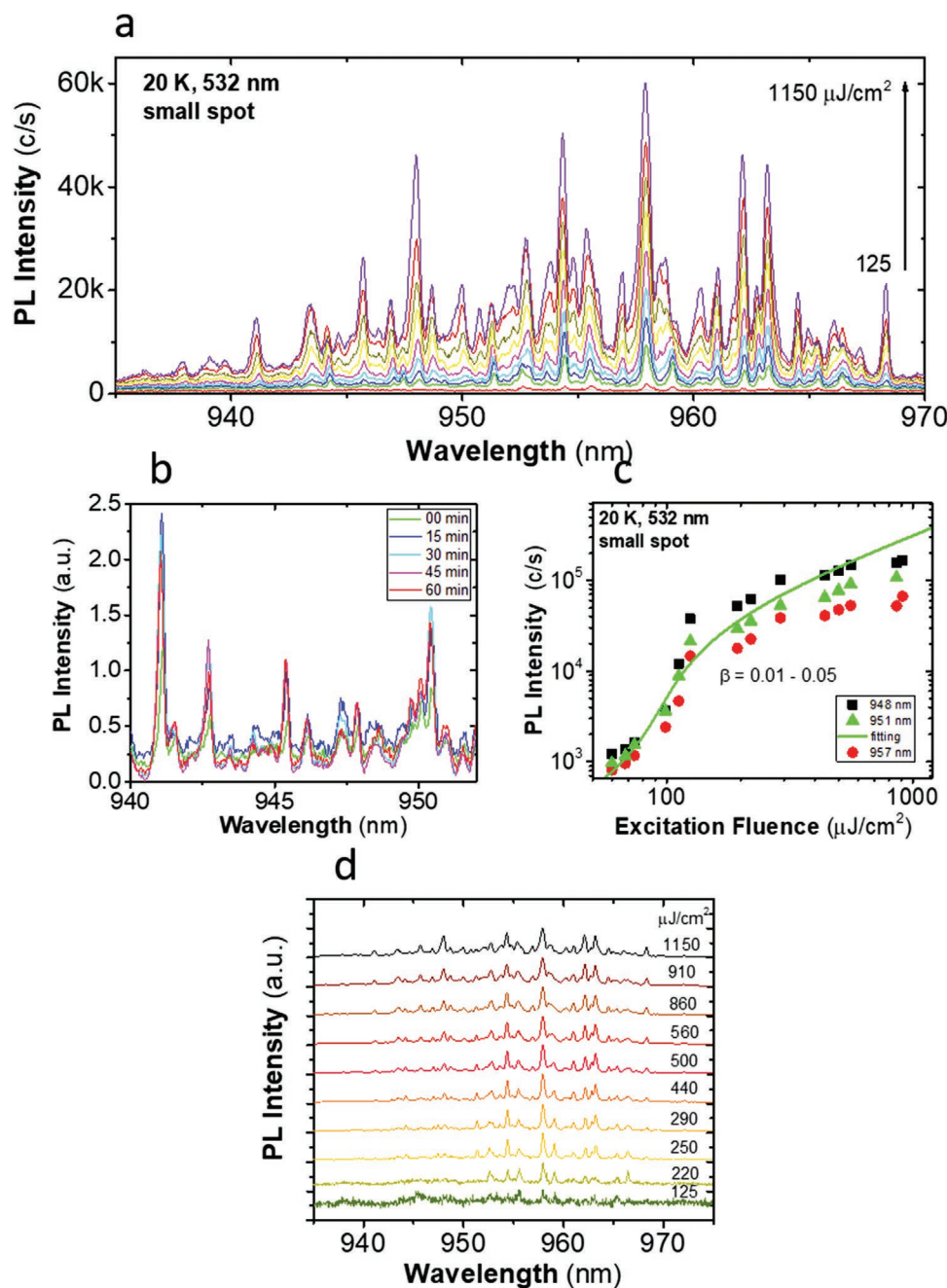
Figure 4. RL spectra of FASnI$_3$ thin film measured at 20 K under small spot excitation by 532 nm pulses: a) spectra at different excitation fluences; b) Spectra at constant excitation fluence recorded each 15 min interval; c) Log–Log presentation of dependence of the intensity of individual RL lines on excitation fluence and the rate equation modeling curve obtained by fitting the data obtained for 951 nm line; d) Same spectra as in (a) but presented in a normalized form with a vertical shift between spectra for a convenience.

samples, and does not depend on the excitation wavelength and spot size, compare wavelength histograms in **Figure 5**. However, it strongly depends on temperature and is ≈0.3–0.5 nm at 20 K, see Figure 5a,b, and 0.8–1.3 nm at 300 K, see Figure 5c,d. Besides, the mode spacing distributions are sufficiently narrow with a clearly defined maximum. All these observations suggest that the so-called *mode repulsion effect* can be responsible for the formation of reproducible RL spectra in FASnI$_3$,[36–40] see below for further discussion.

Finally, we performed also experiments to shed light onto the role of the FASnI$_3$ films morphology on the parameters of the observed RL signals. To do so, we slightly modified the synthetic protocol for obtaining the polycrystalline FASnI$_3$ films, which induced a reduction of the average crystalline grain size, from ≈800–1000 to ≈500 nm, accompanied with the formation of less dense and pinhole-containing films, see Note S2 and Figures S11–S14 (Supporting Information). Such morphological modifications resulted in an increase of the ASE threshold, up

**ADVANCED
SCIENCE NEWS**

www.advancedsciencenews.com

**ADVANCED
MATERIALS**

www.advmat.de
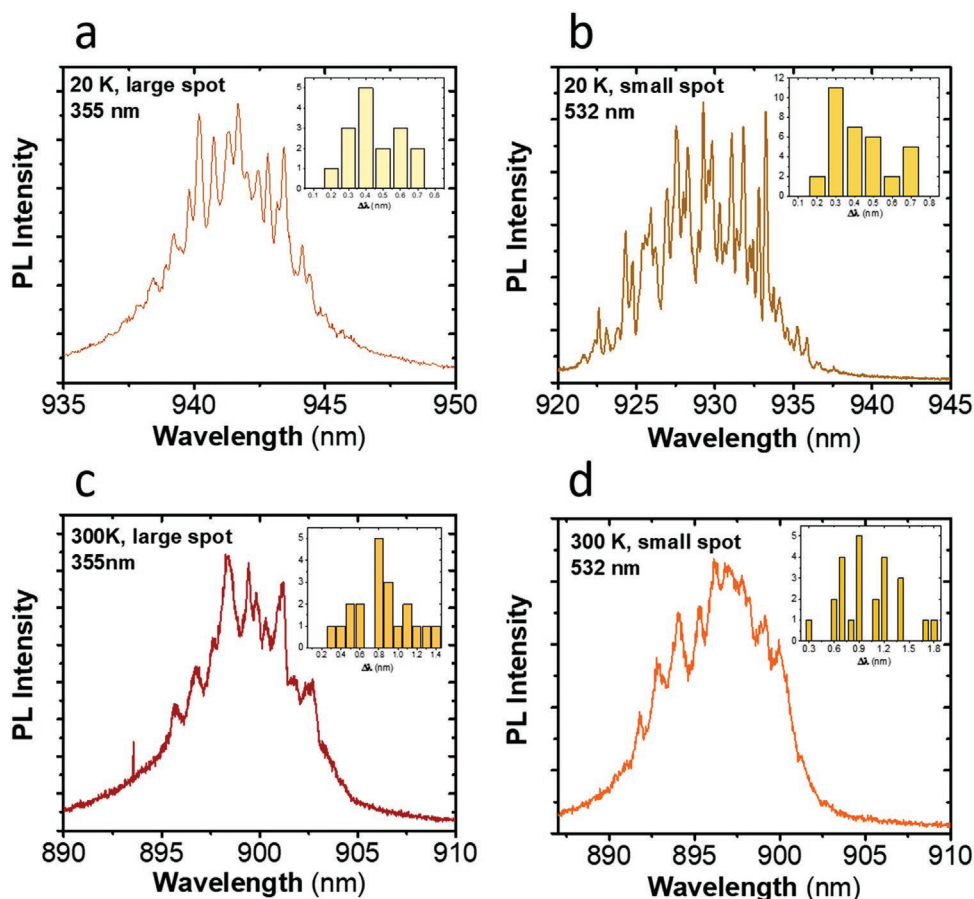
Figure 5. Typical RL spectra measured for FASnI$_3$ films at a,b) 20 K and c,d) 300 K. The corresponding insets are mode spacing distributions, which were constructed on the basis of one presented spectrum for (a,b) and of two-three spectra for (c,d).

to ≈25 µJ cm^{-2} at 20 K, but without any significant change in the quality and stability of the narrow RL lines.

3. Discussion

To understand the mechanisms responsible for the spectral stability of RL modes in FASnI$_3$ films, we will compare their physical and morphological parameters with those of MAPbI$_3$ films investigated under the same conditions. First, it is unlikely that different average size of grains can be the reason of spectral stability for different RL lines. Indeed, as we showed above, changing the average grain size in FASnI$_3$ films from 800 to 500 nm does not affect the spectral stability of RL modes. For the same reasoning, it is unlikely that the 400-nm average grain size in MAPbI$_3$ can be an explanation for the lack of RL modes stability for this material.

The next factor possibly contributing to the observation of high-quality stable RL lines for FASnI$_3$ films, as compared to MAPbI$_3$, is the higher refractive index of the former (n = 2.4) compared to the latter (n = 2.2) in the corresponding PL emission regions.[24,41] From the most general considerations, it is clear that the value of n of the scattering medium determines how efficient is the positive feedback in a random laser: higher

value of n provides stronger feedback. This should certainly affect the value of the RL generation threshold, however, it is difficult to claim straightforwardly that such relatively small change (10%) in the refractive index is responsible for the dramatic increase of the laser modes stability. In addition, the values of n for FASnI$_3$ and MAPbI$_3$ films themselves are far from those magnitudes that are considered in the literature to provide strong spatial localization of laser modes, up to the size of the radiation wavelength, and their stability due to the absence of interaction between them. There are only a few examples of RL systems in the literature, in which the spectral stability of RL modes is ensured precisely by this strong localization mechanism of RL modes. Two of them are purely semiconductor structures, but none of them is a thin layer as we show in this work. First of all, these are films of ZnO nanocrystals, for which spectrally reproducible RL generation under constant pumping was observed with Q ≈10^3.[6] The difference between the refractive index of ZnO and the environment (air) was Δn = 2.0 compared to Δn = 1.4 for FASnI$_3$ relative to air. The second such case was recently observed for InP random nanowire arrays, where refractive index contrast between InP and free space was Δn = 2.46.[42] Finally, one more system with strongly localized stable RL modes was studied, in which the organic dye rhodamine 640 in methanol was used

as a gain material and porous GaP as a scattering medium that resulted in a $\Delta n = 2.06$.[37] In all the cases mentioned, the stability of RL lines was observed, but not studied in detail.

Thus, based on a comparison with the above literature data, we believe that, in the case of FASnI$_3$, the stability of laser modes is unlikely to be ensured by a strong spatial localization of these modes: the refractive index of the material is clearly insufficient for this.

Why do we observe a very clear and reproducible system of narrow laser lines for the FASnI$_3$ film and do not for the MAPbI$_3$ films? Let us briefly recall what causes the absence of spectral reproducibility of RL lines for the vast majority of RL systems. In a scattering optical medium, which has the ability to enhance luminescence under high-power pumping, random resonators appear in the form of closed loops,[4] the resonant wavelength in which, if we represent them in the form of Fabry–Perot resonators, satisfies the interference maximum condition $\lambda_x = 2nL_x/m_x$, where λ_x is the resonant wavelength of the x_{th} resonator, which is inside the gain contour of a material, L_x is the physical length of the x_{th} resonator, n is the refractive index of active medium, and m_x is an integer. If the refractive index of the medium is insufficient for strong spatial localization of laser modes, then these modes can have sizes of tens and hundreds of micrometers on the sample surface, which is usually comparable to the size of the excitation spot.[37] At their initial appearance, the modes can have arbitrarily close resonant frequencies (wavelengths), but the competition between them leaves only the modes with the highest gain. Since all these modes spatially intersect and contain common luminescent centers, this leads to the effect that small random fluctuations in the total energy of the exciting pulses or in the distribution of the pulse energy over the film surface will lead to different final set of "winning" modes.[4]

Why, then, in the case of FASnI$_3$, when the same spatial overlap of all formed random resonators surely takes place, can the generated RL spectra be reproduced from pulse to pulse? Our analysis of the mode spacing distribution for the case of FASnI3 film, Figure 5, led us to the idea that there is a specific mechanism that could provide the mode reproducibility. Indeed, the observed mode spacing distributions in Figure 5 are rather narrow with an explicit maximum. This led us to the conclusion that the distribution of modes in the RL spectrum of FASnI$_3$ films can be controlled by the so-called *mode repulsion effect*, which was earlier observed for a molecular lasing system consisting of inhomogeneously broadened Rhodamine molecules in a polymer as a gain medium and TiO$_2$ microparticles as a scattering component. As qualitative analysis and quantitative model calculations showed, the key parameter of the system, which ensures the spectral stability of the generated RL modes, was the strong inhomogeneous broadening (IB) in the gain medium.[36,39] The mechanism of stabilization of RL modes in systems with strong IB is based on the following. Owing to the large IB of the emitting centers, reproducible lasing can occur simultaneously in modes that are spatially overlapped, as long as the spectral separation between the modes is larger than the homogeneous linewidth of the emitting centers. When this requirement is satisfied, any interaction between the overlapped modes is absent because the different modes do not contain any common luminescent

centers: in IB materials different emission wavelengths correspond to different emission centers. In this way, the absence of interaction between different strongly overlapping modes is ensured.

As some studies reported in the recent years show, emission centers of FASnI$_3$ and other Sn-based perovskites indeed demonstrate IB, in contrast to Pb-based counterparts.[43–45] In the literature, such an IB is associated with a structural disorder in Sn-containing perovskites, and the structural disorder can also manifest itself in a change in the spectral position of the PL spectra depending on the location of the luminescence detection (inhomogeneity of the PL spectra over the sample). We observed just such an effect, and it increases with decreasing temperature, see Figure 1a and Figure S1a (Supporting Information). The distribution in PL maximum position is linked to the octahedral tilting and Sn off-centering within the perovskite lattice, influenced by the procedure used to prepare the material,[43,45] as well as by the poor crystallinity and lattice distortion.[45] As shown in another precedent work,[44] FASnI$_3$ films exhibit a significantly broader emission than is observed for FAPbI$_3$ counterpart: at 4 K, the PL linewidth for FASnI$_3$ is ≈70–110 meV as opposed to ≈20 meV for FAPbI$_3$ and the inhomogeneous width of FASnI$_3$ is evaluated to be ≈63 meV. Our own observations demonstrate that the width of the gain band in FASnI$_3$ films is far superior to that of MAPbI$_3$. Indeed, the spectral range in which RL lines are observed in FASnI$_3$ films at 20 K is ≈50 meV, while the similar range for MAPbI$_3$ films is ≈7 meV, see Figure S14 (Supporting Information). Note that the recently found PL spectrum blue shift and broadening effect in FASnI$_3$ with increasing excitation energy density is also related to the IB induced by the structural disorder.[46,47]

Figure 6 schematically illustrates the proposed stabilization mechanism for RL modes in FASnI$_3$. The modes determined by the random resonator parameters are represented as narrow contours in different colors (dashed lines). The maxima of these contours satisfy the interference maximum condition and have the values $\lambda_x = 2nL_x/m_x$, where λ_x is the resonant wavelength of the x_{th} resonator, which is inside the gain contour of a material, L_x is the physical length of the x_{th} resonator, n is the refractive index of active medium, and m_x is an integer. That is, the spectral modes shown in Figure 6 within the inhomogeneously

$$\lambda_1 = 2nL_1/m_1$$
$$\lambda_2 = 2nL_2/m_2$$
$$\lambda_x = 2nL_x/m_x$$

Wavelength
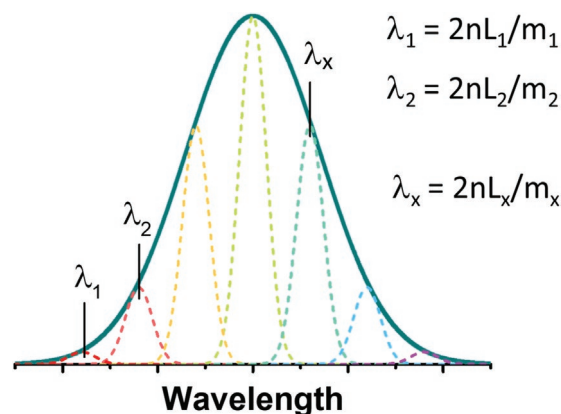
Figure 6. The mechanism of generation of reproducible RL modes (narrow dashed contours) under conditions of inhomogeneously broadened amplification contour (sold line). See the text for further details.

broadened contour (solid line) correspond to 7 resonators with slightly different values of the resonator optical length $2nL_x$ and the number m_x, but all the resonators are well overlapped in space and have a size, which is commensurate with excitation spot size. In this case, each of the modes is coupled to the population of only its subgroup of emitting centers, and these subgroups, which emit luminescence at different wavelengths, do not interact with each other, thus ensuring the spectral stability of the generated modes. All modes compete with each other for the opportunity to be spectrally located as close as possible to the maximum of the gain contour. As a result, the modes are located at the minimum possible spectral distance from each other, which is determined by the homogeneous broadening of the individual modes. As soon as the homogeneous width grows with temperature, the mode spacing increases, as it is experimentally found, see Figure 5. Note that the mode stability condition in the above mechanism requires a spectral distance between modes ($h\Delta\nu_{dist}$) of at least two widths of the uniformly broadened luminescence band ($h\Delta\nu_{hom}$),[36,39] which is actually satisfied in our case. Indeed, at 20 K the average mode spacing is ≈0.4 nm (0.6 meV), while $h\Delta\nu_{hom}$ is comprised within 0.1–0.5 meV, upon the influence of the spectral diffusion broadening mechanism, as reported in the literature for the micro-PL linewidth measured in single nanocrystals of lead iodide perovskites.[48]

4. Conclusions

Unusual spectrally stable, low-threshold and non-chaotic RL with a quality factor Q as high as ≈10^4 is observed at 20 K for polycrystalline FASnI$_3$ thin films and it is also observed at room temperature, but with the reduction of Q in one order of magnitude. In fact, it is the first time, to the best of our knowledge, that this behaviour is observed in semiconductor thin films. These results are interestingly in contrast with those obtained for MAPbI$_3$ films, where only ineffective RL with non-reproducible spectral positions of modes was found at low temperature and it is not observed at room temperature. In principle, the only essential difference in optical properties among the Sn- and Pb-based perovskites is a huge inhomogeneous broadening (IB) of emitting centres of the former compound, and namely this IB turns to be responsible for the mechanism that rules the stabilisation of the RL modes. Thus, the unusual large IB, which is considered as a serious drawback of Sn-based perovskites for the manufacturing of solar cells that leads to deleterious efficiency losses, turns out to be a key property that allows creating reproducible sources of narrow laser spectral lines based on inexpensive random lasers.

Therefore, we can speculate that this work opens pioneering prospects for fabrication of high-Q and spectrally reproducible coherent random lasers, with even sufficiently high directionality, for example by deposition of FASnI$_3$ film on a fiber facet.[49] It also seems promising to create high-Q electrically-driven random[50–54] and whispering gallery mode[55] lasers on the basis of FASnI$_3$ films. Finally, the discovered mechanism of RL self-induced reproducibility can be extended to other semiconductor systems with IB, such as ensembles of quantum-confined quantum dots with a wide size distribution,

which remarkably widens the repercussion of this work in the fields of photonics and applied physics.

Supporting Information

Acknowledgements

Conflict of Interest

The authors declare no conflict of interest.

Data Availability Statement

The data that support the findings of this study are available from the corresponding author upon reasonable request.

Keywords

[1] M. Leonetti, C. Conti, C. Lopez, *Nat. Photonics* **2011**, *5*, 615.
[2] R. C. Polson, M. E. Raikh, Z. V. Vardeny, *C. R. Physique* **2002**, *3*, 509.
[3] H. Cao, *Mult. Scattering Waves Random Media, Proc. U.S. Army Workshop* **2003**, *13*, R1.
[4] H. Cao, *J Phys A Math Gen* **2005**, *38*, 10497.
[5] H. Cao, Y. G. Zhao, H. C. Ong, S. T. Ho, J. Y. Dai, J. Y. Wu, R. P. H. Chang, *Appl. Phys. Lett.* **1998**, *73*, 3656.
[6] H. Cao, Y. G. Zhao, S. T. Ho, E. W. Seelig, Q. H. Wang, R. P. H. Chang, *Phys. Rev. Lett.* **1999**, *82*, 2278.
[7] S. Colella, E. Mosconi, P. Fedeli, A. Listorti, F. Gazza, F. Orlandi, P. Ferro, T. Besagni, A. Rizzo, F. Calestani, G. Gigli, F. De Angelis, R. Mosca, *Chem. Mater.* **2013**, *25*, 4613.
[8] F. Brivio, A. B. Walker, A. Walsch, *APL Mater.* **2013**, *1*, 042111.
[9] S. De Wolf, J. Holovsky, S.-J. Moon, P. Löper, B. Niesen, M. Ledinsky, F.-J. Haug, J.-H. Yum, C. Ballif, *J. Phys. Chem. Lett.* **2014**, *5*, 1035.
[10] G. Xing, N. Mathews, S. S. Lim, N. Yantara, X. Liu, D. Sabba, M. Gratzel, S. Mhaisalkar, T. C. Sum, *Nat. Mater.* **2014**, *13*, 476.
[11] R. Dhanker, A. N. Brigeman, A. V. Larsen, R. J. Stewart, J. B. Asbury, N. C. Giebink, *Appl. Phys. Lett.* **2014**, *105*, 151112.
[12] M. L. De Giorgi, M. Anni, *Appl. Sci.* **2019**, *9*, 4591.
[13] Z. Hu, Z. Liu, Z. Zhan, T. Shi, J. Du, X. Tang, Y. Leng, *Adv. Photonics* **2021**, *3*, 034002.
[14] Z.-F. Shi, X.-G. Sun, D. Wu, T.-T. Xu, Y.-T. Tian, Y.-T. Zhang, X.-J. Li, G.-T. Du, *J. Mater. Chem. C* **2016**, *4*, 8373.

**ADVANCED
SCIENCE NEWS**

www.advancedsciencenews.com

**ADVANCED
MATERIALS**

www.advmat.de

[15] T. S. Kao, Y.-H. Chou, K.-B. Hong, J.-F. Huang, C.-H. Chou, H.-C. Kuo, F.-C. Chen, T.-C. Lu, *Nanoscale* **2016**, *8*, 18483.

[16] A. Safdar, Y. Wang, T. F. Krauss, *Opt. Express* **2018**, *26*, A75.

[17] Y.-C. Wang, H. Li, Y.-H. Hong, K.-B. Hong, F.-C. Chen, C.-H. Hsu, R.-K. Lee, C. Conti, T. S. Kao, T.-C. Lu, *ACS Nano* **2019**, *13*, 5421.

[18] Z. Y. Wu, B.-L. Jian, C.-S. Wu, H.-C. Hsu, *Opt. Express* **2020**, *28*, 21805.

[19] R. Wang, J. Wang, S. Tan, Y. Duan, Z.-K. Wang, Y. Yang, *Trends Chem* **2019**, *1*, 368.

[20] K. J. Savill, A. M. Ulatowski, L. M. Herz, *ACS Energy Lett.* **2021**, *6*, 2413.

[21] G. Xing, M. H. Kumar, W. K. Chong, X. Liu, Y. Cai, H. Ding, M. Asta, M. Grätzel, S. Mhaisalkar, N. Mathews, T. C. Sum, *Adv. Mater.* **2016**, *28*, 8191.

[22] Z. Y. Wu, Y. Y. Chen, L.-J. Lin, H.-C. Hsu, *J. Phys. Chem. C* **2021**, *125*, 5180.

[23] J. Sánchez-Diaz, R. S. Sánchez, S. Masi, M. Krečmarova, A. O. Alvarez, E. M. Barea, J. Rodriguez-Romero, V. S. Chirvony, J. F. Sánchez-Royo, J. P. Martinez-Pastor, I. Mora-Seró, *Joule* **2022**, *6*, 861.

[24] I. Suárez, V. S. Chirvony, J. Sánchez-Díaz, R. S. Sánchez, I. Mora-Seró, J. P. Martínez-Pastor, *Adv. Opt. Mater.* **2022**, *10*, 2200458.

[25] J. Q. Grim, S. Christodoulou, F. Di Stasio, R. Krahne, R. Cingolani, L. Manna, I. Moreels, *Nat. Nanotechnol.* **2014**, *9*, 891.

[26] J. Andreasen, A. Asatryan, L. Botten, M. Byrne, H. Cao, L. Ge, L. Labonté, P. Sebbah, A. Stone, H. Türeci, C. Vanneste, *Adv. Opt. Photonics* **2011**, *3*, 88.

[27] S. Shao, J. Liu, G. Portale, H.-H. Fang, G. R. Blake, G. H. ten Brink, L. J. A. Koster, M. A. Loi, *Adv. Energy Mater.* **2018**, *8*, 1702019.

[28] P. Liu, X. He, J. Ren, Q. Liao, J. Yao, H. Fu, *ACS Nano* **2017**, *11*, 5766.

[29] R. Agarwal, C. J. Barrelet, C. M. Lieber, *Nano Lett.* **2005**, *5*, 917.

[30] R. Chen, B. Ling, X. W. Sun, H. D. Sun, *Adv. Mater.* **2011**, *23*, 2199.

[31] K. Wang, S. Sun, C. Zhang, W. Sun, Z. Gu, S. Xiao, Q. Song, *Mater. Chem. Front.* **2017**, *1*, 477.

[32] Y.-H. Hong, T. S. Kao, *Nanoscale Adv* **2020**, *2*, 5833.

[33] J. Navarro-Arenas, I. Suárez, A. F. Gualdrón-Reyes, I. Mora-Seró, J. Bisquert, J. P. Martínez-Pastor, *Adv. Opt. Mater.* **2021**, *9*, 2100807.

[34] A. E. Siegman, *Lasers*, University Science Books, Mill Valley **1986**, Secs. 13.2 and 13.3.

[35] H. Yokoyama, S. D. Brorson, *J. Appl. Phys.* **1989**, *66*, 4801.

[36] H. Cao, X. Jiang, Y. Ling, J. Y. Xu, C. M. Soukoulis, *Phys. Rev. B* **2003**, *67*, 161101(R).

[37] K. L. van der Molen, R. W. Tjerkstra, A. P. Mosk, A. Lagendijk, *Phys. Rev. Lett.* **2007**, *98*, 143901.

[38] X. Jiang, C. M. Soukoulis, *Phys. Rev. Lett.* **2000**, *85*, 70.

[39] X. Jiang, S. Feng, C. M. Soukoulis, J. Zi, J. D. Joannopoulos, H. Cao, *Phys. Rev. B* **2004**, *69*, 104202.

[40] O. Zaitsev, L. Deych, *J Opt* **2010**, *12*, 024001.

[41] M. Anaya, J. P. Correa-Baena, G. Lozano, M. Saliba, P. Anguita, B. Roose, A. Abate, U. Steiner, M. Grätzel, M. E. Calvo, A. Hagfeldt, H. Míguez, *J. Mater. Chem. A* **2016**, *4*, 11214.

[42] M. Rashidi, H. H. Tan, S. Mokkapati, *Optica* **2021**, *8*, 1160.

[43] A. G. Kontos, A. Kaltzoglou, M. K. Arfanis, K. M. McCall, C. C. Stoumpos, B. W. Wessels, P. Falaras, M. G. Kanatzidis, *J. Phys. Chem. C* **2018**, *122*, 26353.

[44] S. Kahmann, S. Shao, M. A. Loi, *Adv. Funct. Mater.* **2019**, *29*, 1902963.

[45] D. Di Girolamo, E. Blundo, G. Folpini, C. Ponti, G. Li, M. H. Aldamasy, Z. Iqbal, J. Pascual, G. Nasti, M. Li, R. Avolio, O. Russina, F. Alharthi, M. Felici, A. Petrozza, A. Polimeni, A. Abate, *Sol. RRL* **2022**, *6*, 2100825.

[46] K. J. Savill, M. T. Klug, R. L. Milot, H. J. Snaith, L. M. Herz, *J. Phys. Chem. Lett.* **2019**, *10*, 6038.

[47] H.-H. Fang, S. Adjokatse, S. Shao, J. Even, M. A. Loi, *Nat. Commun.* **2018**, *9*, 243.

[48] H. Pashaei Adl, S. Gorji, G. Muñoz-Matutano, R. I. Sánchez-Alarcón, R. Abargues, A. F. Gualdrón-Reyes, I. Mora-Seró, J. P. Martínez-Pastor, *J. Lumin.* **2021**, *240*, 118453.

[49] X. Zhang, S. Yan, J. Tong, X. Shi, S. Zhang, C. Chen, Y. Y. Xiao, C. Han, T. Zhai, *Nanophotonics* **2020**, *9*, 935.

[50] X. Ma, P. Chen, D. Li, Y. Zhang, D. Yang, *Appl. Phys. Lett.* **2007**, *91*, 251109.

[51] S. F. Yu, *J. Phys. D: Appl. Phys.* **2015**, *48*, 483001.

[52] F. Gao, M. M. Morshed, S. B. Bashar, Y. Zheng, Y. Shi, J. Liu, *Nanoscale* **2015**, *7*, 9505.

[53] A. Consoli, N. Caselli, C. López, *Nat. Photonics* **2022**, *16*, 219.

[54] T.-L. Shen, H.-W. Hu, W.-J. Lin, Y.-M. Liao, T.-P. Chen, Y.-K. Liao, T.-Y. Lin, Y.-F. Chen, *Sci. Adv.* **2020**, *6*, eaba1705.

[55] S. B. Bashar, C. Wu, M. Suja, H. Tian, W. Shi, J. Liu, *Adv. Opt. Mater.* **2016**, *4*, 2063.